HHS Public Access

Author manuscript

Ann Biomed Eng. Author manuscript; available in PMC 2018 September 01.

Published in final edited form as:

Ann Biomed Eng. 2017 September ; 45(9): 2098–2108. doi:10.1007/s10439-017-1867-8.

Enhancement of Energy Production of the Intervertebral Disc by the Implantation of Polyurethane Mass Transfer Devices

Yu-Fu Wang, MS[1], **Howard B. Levene, MD, PhD**[2], **Weiyong Gu, PhD**[3], and **C.-Y. Charles Huang, PhD**[1]

[1]Department of Biomedical Engineering, College of Engineering, University of Miami, Coral Gables, FL

[2]Department of Neurological Surgery, University of Miami Miller School of Medicine, Miami, FL

[3]Department of Mechanical and Aerospace Engineering, College of Engineering, University of Miami, Coral Gables, FL

Abstract

Insufficient nutrient supply has been suggested to be one of the etiologies for intervertebral disc (IVD) degeneration. We are investigating nutrient transport into the IVD as a potential treatment strategy for disc degeneration. Most cellular activities in the IVD (e.g., cell proliferation and extracellular matrix production) are mainly driven by adenosine-5′-triphosphate (ATP) which is the main energy currency. The objective of this study was to investigate the effect of increased mass transfer on ATP production in the IVD by the implantation of polyurethane (PU) mass transfer devices. In this study, the porcine functional spine units were used and divided into intact, device and surgical groups. For the device and surgical groups, two puncture holes were created bilaterally at the dorsal side of the annulus fibrosus (AF) region and the PU mass transfer devices were only implanted into the holes in the device group. Surgical groups were observed for the effects of placing the holes through the AF only. After 7 days of culture, the surgical group exhibited a significant reduction in the compressive stiffness and disc height compared to the intact and device groups, whereas no significant differences were found in compressive stiffness, disc height and cell viability between the intact and device groups. ATP, lactate and the proteoglycan contents in the device group were significantly higher than the intact group. These results indicated that the implantation of the PU mass transfer device can promote the nutrient transport and enhance energy production without compromising mechanical and cellular functions in the disc. These results also suggested that compromise to the AF has a negative impact on the IVD and must be addressed when treatment strategies are considered. The results of this study will help guide the development of potential strategies for disc degeneration.

Introduction

Low back pain affects up to 85% of people in their lifetimes. This contributes to healthcare costs in the United States which exceeds $100 billion per year [1, 2]. One major cause of

Corresponding Author: C.-Y. Charles Huang, PhD 1251 Memorial Dr #219, Coral Gables, FL 33146, Phone: (305)284-1320, Fax: (305)284-6494, c.huang1@miami.edu.

low back pain is believed to be related to the degeneration of the intervertebral disc (IVD) [3, 4]. Since the IVD is the largest avascular tissue in human body, insufficient nutrient supply has been suggested to be one of the etiologies for disc degeneration [5, 6]. There are two major pathways for transport of nutrients into the IVD [7, 8]. The annulus fibrosus (AF) receives nutrients from capillaries in the soft tissues that surround at the edges of AF [9, 10]. The vertebral blood vessels are the main nutrient sources for the central region of the IVD which is the nucleus pulposus (NP) [11, 12]. The exchange of nutrients and metabolites in the IVD are mainly driven by concentration gradients [13]. This results in the central region of the IVD having lower levels of oxygen, glucose and other nutrients compared to the outer region [14, 15]. As long as the nutrient level remains above a vital threshold, the viability and functionality of the IVD can be maintained. When nutrient demand exceeds supply, it results in decreased cell activity level and may ultimately cause cell death [16, 17]. It is observed that calcification of the vertebral endplate with age causes a reduction in the nutrient level in the NP region [18–20]. This loss of nutrients is detrimental to cellular functions such as extracellular matrix (ECM) production and may ultimately result in disc degeneration. Addressing and supplementing nutrient supply could be one of the potential treatment strategies for treating or reversing disc degeneration.

Most of the cell activities in the IVD such as ECM production and maintenance are high energy demanding processes which require adenosine-5′-triphosphate (ATP) as fuel [21]. ATP also serves as a building block in the formation of UDP-sugars and 3′-phosphoadenosine 5′-phosphosulphate (PAPS) for biosynthesis of proteoglycans (PG) [22, 23] which are one of the major ECM components in the IVD. Additionally, ATP is an extracellular signaling molecule that mediates a variety of cellular activities through purinergic signal pathways [24–26]. Our previous study demonstrated that mechanical loading promotes ATP production and release from IVD cells [27] while extracellular ATP can modulate the ECM biosynthesis of IVD cells [28]. Since ATP plays an important role in maintaining the integrity and function of the IVD, chronic malnourishment and loss of ATP concentration may lead to cell death and ultimately IVD degeneration.

Recent studies have shown that several biomaterials implanted for closure of AF defects maintain the height and stability of the IVD [29–31]. Since there are ample nutrient supplies at the edges of AF due to blood supply, porous materials with high transport properties implanted in AF can be designed to facilitate transport of nutrients from the edge of AF into the NP region in order to promote cellular energy production. In addition, the importance of matching AF mechanical properties has been emphasized on developing successful biomaterials for AF repair [32]. Our previous study has systematically characterized the relationships between the transport and mechanical properties of polyurethane (PU) porous scaffolds and demonstrated that the PU porous scaffolds can exhibit higher transport properties and similar mechanical strength compared to AF tissues [33]. Therefore, the objective of this study was to investigate the enhancement of ATP production in the IVD by the implantation of porous PU scaffolds in the AF as a passive mass transfer device.

Materials and Methods

Fabrication of PU mass transfer devices

The PU (polyurethane) mass transfer device was fabricated by a salt leaching/phase inversion method based on our previous study [33, 34]. The procedure is as follows: a PU solution of 25% (w/v) was prepared by dissolving PU pellets (Tecflex® SG-85A, Lubrizol, Wickliffe, OH) in N,N-dimethyl formamide (DMF; Sigma-Aldrich, St. Louis, Mo). Sodium chloride (NaCl; Sigma-Aldrich) crystals were ground and sieved to select sizes smaller than 70 μm and were mixed with the PU solution at 9/1 (NaCl/PU) weight ratios. Polytetrahydrofuran (Sigma-Aldrich) was also added to the NaCl-PU mixture in 25% (v/v) volume ratio as a soluble filler to enhance the interconnectivity of the porous scaffolds. The mixed solution was well stirred and then injected into glass cylinder molds. Porous PU scaffolds were formed by submerging the cylinder molds in 65% of ethanol with 1% DMF via phase inversion for 48 hours. After separating from the molds, the porous PU scaffolds were rinsed in distilled water for 24 hours in order to remove NaCl crystals. After the rinsing step, the porous PU scaffolds (diameter: 2.5 mm, long: 25 mm) were preserved in PBS and utilized as mass transfer devices for the further experiments. The device length of 25 mm was chosen because of sufficient length (8 mm) in NP region and better manipulation during the insertion procedure.

Mass transfer device experiment

The lumbar spines were obtained from Yorkshire pigs of both sexes (age: 14~16 weeks; weight: 80~100 lbs.) within 2 hours of sacrifice (Department of Veterinary Resource, Miami, FL). Three functional spine units (FSUs) (L2 to L5) were isolated from each pig by making transverse cuts through the vertebrae by a sterile bone saw. The sectioned planes of vertebrae were sealed with bone cement (P.A.R. Brand Acrylic Resin, Wheeling, IL) in order to block nutrient diffusion pathway through endplate route and to simulate endplate calcification conditions. After washing with PBS containing 10% of antibiotic-antimycotic (Lonza, Walkersville, MD) and 100 μg/ml of gentamicin sulfate (Lonza) for 3 times, the FSUs from each pig were randomly divided into 3 experimental groups: intact, device, and surgical groups. For the device and surgical groups, two puncture holes (diameter smaller than 2.5 mm) were created bilaterally using sterile needles at the dorsal side of the AF region without removing tissue. The PU mass transfer devices were squeezed and implanted under a press-fit condition in the device group only (Figure 1a). All of the experimental groups were cultured in low glucose (1g/L) Dulbecco’s Modified Eagle Medium (DMEM, Invitrogen, Carlsbad, CA) containing 1% of antibiotic-antimycotic and 50 μg/ml of gentamicin sulfate. After 7 days of culture, a transverse cut was made at the mid-disc height of the FSUs to expose the NP and AF regions. Tissue samples (~25mg) were harvested from three different locations (AF, peripheral NP and central NP regions) along PU mass transfer devices in the device group and the same locations in the intact group (Figure 1b). Additionally, the sealing effect of PU mass transfer devices was examined before and after 7 days of culture. The FSUs with implantation of PU transfer device were incubated in the PBS containing 1 mg/ml Fluorescein (Sigma-Aldrich) for 36 hours. A transverse cut was made at mid height of the FSU and fluorescence images were captured using the BioSpectrum imaging system (UVP, Upland, CA).

Disc height measurement

The disc height of each group (n=11) was measured from endplate to endplate at 3 different random locations by a digital caliper (Mitutoyo 500-196-20, Aurora, IL, accuracy ± 0.025 mm) before and after 7 days of culture.

Mechanical testing

Uniaxial compressive tests were performed to determine the compressive structural stiffness of the IVD before and after 7 days of culture based on the protocol described previously [30]. A custom-made loading system developed in our laboratory [27] was used for the compressive tests. The FSUs from each groups (n=8) were first applied with a compressive preload of 0.5 kg, followed by a dynamic compressive strain of 5% with a frequency of 0.1 Hz. The 25^{th} loading cycle was used to determine the compressive stiffness which was calculated by a linear regression of the load-displacement curve between 60% and 100% of the maximal load [30].

Glucose measurement

The tissue samples harvested from the intact and device groups were analyzed for glucose concentration (n=8). Tissue samples (~25 mg) were boiled for 5 minutes with 500 μl of 3 mM EDTA (Sigma-Aldrich). After addition of 500 μl PBS solution containing 250 μg/ml of papain (Sigma-Aldrich) and 10 mM of EDTA, the samples were incubated in the heater at 65°C for 16 hours [35]. Next, the glucose concentration was measured by the glucose (GO) assay kit (Sigma-Aldrich). The tissue digestion solutions of 50 μl were first mixed with 100 μl of the assay reagent and incubated at 37 °C for 30 mins. After the incubation, 100 μl of sulfuric acid (VWR, Radnor, PA) was added and the absorbance was measured at 540 nm by a multimode detector (DTX880, Beckman Coulter, Brea, CA). Tissue density was measured using a density determination kit and an analytical balance (Sartorius, Germany) for calculation of tissue volume [36]. Glucose concentration was calculated by dividing the glucose content by tissue volume.

Cell viability

The tissue samples (n=5) from peripheral NP location in the intact and device groups were analyzed for cell viability. The Hoechst 33258 dye (Polysciences, Warrington, PA.) was used to identify the total number of cells and ethidium homodimer-1 (Biotium, Fremont, CA) was used for dead cell staining [37]. The images were analyzed by ImageJ software for cell counting.

ATP measurement

A modified phenol extraction method combining the luciferin-luciferase assay (Sigma-Aldrich) were utilized for ATP measurement (n=13) [38]. Tissue samples (~25 mg) from peripheral NP location in the intact and device groups were first homogenized with 500 μl of water saturated phenol (Sigma-Aldrich), and then mixed with 500 μl of chloroform (Sigma-Aldrich) and 300 μl of de-ionized water. The mixed solution was thoroughly shaken for 20 secs and centrifuged at 13000 rpm for 10 min at 4 °C. The supernatants were diluted 1000-

fold with de-ionized water and mixed with the assay reagent with 1 to 9 volume ratio and the luminescence was measured immediately by the multimode detector.

Lactate measurement

Lactate measurement was based on the protocol described in our previous study (n=13) [39]. A lactate reaction reagent was made by dissolving 5 mg/mL of β-nicotineamide adenine dinucleotide (Sigma-Aldrich), 0.2 M glycine buffer (Sigma-Aldrich) and 22.25 units/mL of L-lactic dehydrogenase (Sigma-Aldrich) in de-ionized water. Tissue samples (~25 mg) from peripheral NP location in the intact and device groups were digested with papain as described in the section of glucose measurement. The tissue digestion solutions were mixed with the lactate reaction reagent with 1 to 1 volume ratio, and the absorbance of 340 nm was measured by the multimode detector.

PG measurement

PG content was quantified by using the dimethylmethylene blue (DMMB) dye-binding assay which was described in our previous study (n=13) [28]. Tissue samples (~25 mg) from peripheral NP location in the intact and device groups were digested with papain as described in the section of glucose measurement. The tissue digestion solutions were diluted 11-fold with deionized water and mixed with DMMB dye solution with 1 to 20 volume ratio, and the absorbance of 525 nm was measured by the multimode microplate reader (SpectraMAx M2, Molecular Device, Sunnyvale, CA). The PG content was normalized by tissue weight.

DNA measurement

The extraction and digestion solutions for ATP and lactate measurements were also examined for DNA content (n=13). The Hoechst 33258 fluorometric assay was used for the DNA content measurement [35]. In brief, 20 μl of sample solution was first mixed with 200 μl of working solution which contained 0.15 μg/ml of Hoechst dye, 100 mM Tris (Bio-Rad, Hercules, CA), 1 mM EDTA and 0.2 M NaCl. The DNA content was measured by the multimode microplate reader with excitation at 365 nm and emission at 458 nm.

Statistical analysis

A one-way ANOVA followed by a Bonferroni post-hoc test was performed to analyze differences in compressive stiffness reduction and disc height changes among three experimental groups. A paired t-test was also performed to analyze differences in disc height changes of each experimental group before and after 7 days of culture. For glucose concentration, a one-way ANOVA followed by a Bonferroni post-hoc test was also performed to analyze the differences among harvest locations. The ATP and lactate contents were normalized by the DNA content, and then each of device groups was normalized by its respective intact group. The student's t-test was performed to analyze differences in glucose concentration, cell viability, and ATP, lactate, PG and DNA contents between the intact and device group. The statistical analyses were performed using SPSS software (IBM, Chicago, IL). A $p < 0.05$ was considered statistically significant.

Results

Tissue-device sealing condition

After 7 days of culture, the length of PU mass transfer device outside the AF region remained 10 mm which represented no extrusion was observed (Figure 2a). In the sealing test, the results from day 0 and 7 showed that fluorescent solution diffused into the disc via the PU mass transfer device and there was no leaking at the boundary between the device and AF region after 36 hours of incubation (Figure 2b). The puncture holes in device group were still tightly sealed by the PU mass transfer devices.

Disc height

A significant increase in disc height was seen in the intact and device groups (9.04 ± 7.64 % and 5.63 ± 5.78 %, respectively) whereas disc height significantly decreased in the surgical group (−2.99 ± 4.06 %) (intact and device: $p < 0.01$; surgical: $p = 0.032$). When comparing disc height change among three experimental groups, the surgical group was significantly ($p < 0.01$) different from other two groups whereas no statistical difference was found between the intact and device groups (Figure 3e).

Compressive stiffness

Generally, the compressive stiffness was reduced for three experimental groups after 7 days of culture (Figure 3 and Table 1). When comparing among three groups, a significant reduction was found in surgical group (47.8 ± 14.8 %) (surgical-intact: $p = 0.012$; surgical-device: $p = 0.019$). In addition, there was no statistical difference between the intact and device groups. (29.7 ± 9.5 % and 30.8 ± 8.2 %, respectively) (Figure 3a–d).

Glucose concentration

The glucose concentration at central NP, peripheral NP and AF region was showed in figure 4. A gradually decreasing of glucose concentration from AF to central NP region was found in both experiment groups. There was no statistical difference between intact and device groups at three harvest locations after 7 days of culture. However, a slight increase of glucose concentration was still exhibited at NP region in device group.

Cell viability and DNA content

No significant differences were found in cell viability staining between the intact and device groups (90.14 ± 2.73 % and 89.16 ± 2.22 %, respectively) with both groups showing high cell viability after 7 days of culture (Figure 5). Similar DNA contents were found in tissue samples using the phenol and papain extraction methods. No statistical differences were seen in DNA content between the intact and device groups (phenol: 1 ± 0.42 and 0.98 ±0.44; papain: 1 ± 0.42 and 0.97 ± 0.45, respectively).

ATP, lactate and PG contents

With PU mass transfer device implanted for 7 days, the ATP content in the NP region was significantly higher in the device group than the intact group (intact: 1 ± 0.55; device: 2.71 ± 1.83) ($p < 0.01$) (Figure 6a). Similarly, the device group exhibited significantly higher

lactate (intact: 1 ± 0.46; device: 1.93 ± 0.92) and PG contents (intact: 33.41 ± 5.73 μg/mg; device: 37.69 ±2.3 μg/mg) in the NP region than the intact group (lactate: $p < 0.01$; PG: $p = 0.024$) (Figure 6b and 6c).

Discussion

This study investigated the effect of PU mass transfer device implantation on the metabolism of ATP and ECM in the porcine IVD after 7 days of culture. It was found that implantation of PU mass transfer devices increased the production of ATP and PG in the IVD while avoiding negative effects of the PU mass transfer devices on the structural stiffness and height of the IVD. This is the first study to demonstrate the feasibility of enhancing the production of energy and ECM in the IVD by implanting porous mass transfer devices through the AF.

ATP not only serves as an energy source but also a building block for PG biosynthesis [22, 23]. The activities of maintenance and repair of articular cartilage ECM are strongly associated with cell energy storage while the ECM biosynthesis rates are closely related to the availability of ATP [40, 41]. Johnson et al. has reported that intracellular ATP levels decline during the development of spontaneous knee osteoarthritis in guinea pigs, indicating that depletion of ATP is associated with cartilage degeneration [42]. Furthermore, our previous study showed that extracellular ATP promotes the ECM production of IVD cells in agarose gel culture [28]. Those results suggested that ATP production may play an important role in maintaining the healthy ECM structure of the IVD. In this study, with the implantation of PU mass transfer device, the ATP and PG contents were found to be significantly increased at NP region, suggesting that implanting porous mass transfer devices can promote nutrient transport and enhance ATP and ECM production, which has the potential to slow down disc degeneration.

Glycolysis is the process that the cells breakdown glucose into pyruvate and produce ATP. During aerobic conditions, pyruvate enters the mitochondria and more ATP is produced by the Krebs cycle and the electron transport chain. In the anaerobic respiration pathway, pyruvate is oxidized into lactate without ATP production. Previous studies have suggested that ATP is predominantly generated in IVD cells by glycolysis due to hypoxic conditions in the IVD [18, 43, 44]. In this study, both ATP and lactate contents were found to be significantly higher at the peripheral NP region in the device group compared to the intact group, suggesting that the increase in ATP content results from the augmentation of the glycolysis process. In addition, the glucose consumption rate can be described by the Michaelis-Menten Kinetics [44] in which the glucose consumption is highly sensitive to glucose concentration at low glucose levels. It explains that the device group exhibited 2.7 fold higher ATP content with only a slight increase in glucose concentration compared to the intact group.

Previous animal studies showed that needle puncture injury significantly altered the mechanical properties of the IVD and resulted in degenerative changes when the ratio of the needle diameter to disc height is greater than 0.4 [45–47]. A large needle puncture may cause the change of mechanical behaviors of IVD by damaging the AF structure and

depressurizing the NP. Changes in the mechanical microenvironment may also result in degenerative responses in IVD cells, such as catabolic, apoptotic and inflammatory activities [48–51]. In this study, the ratio of the needle diameter to disc height was greater than 0.4. When comparing the structural stiffness and disc height among experimental groups after 7 days of culture, significant reductions in disc height and structural stiffness were found in the surgical group which had defects created in the AF without implantation of mass transfer devices. The findings of the loss of disc height and structural stiffness are consistent with previous studies [30, 45]. In the device group, there was some loss of height, but minimized compared to the surgical groups. Therefore, proper repair of AF structural damage could maintain the mechanical function of the IVD and prevent or slow the development of disc degeneration. Likhitpanichkul et al. has demonstrated on bovine IVDs that sealing large AF defects by fibrin-genipin hydrogel can diminish the NP depressurization and restore the integrity of the AF structure [30]. Similarly, in our study, the PU mass transfer device serves a sealant or plug which repairs AF damage caused by the impanation procedure and maintains the mechanical function of the IVD.

Since there is generally an inverse relationship between the mechanical and transport properties of porous materials [33], seeking the balance between those properties is the key to developing mass transfer devices for the IVD. In our previous study, the mechanical and mass transport properties of the PU mass transfer device have been systematically characterized [33]. With the current fabrication protocol, the compressive modulus of the PU mass transfer device is about 0.15 MPa which is similar to the aggregate modulus of porcine AF tissue [52]. Since an AF defect can alter the local mechanical environment [53], which may have a negative influence on IVD cells at the defect region [48], one of design criteria of biomaterials for repairing IVD is mechanical similarity to native IVD [32]. Therefore, with the mechanical strength similar to the AF, the PU mass transfer device used in this study may minimize the mechanical effects of an AF defect on IVD cells. In addition, the permeability and glucose diffusivity of the PU mass transfer device are about 10^6 and 5 times higher than intact AF tissue respectively [54]. With a higher diffusivity, the PU mass transfer device provides a minimally restricted route for nutrients to diffuse into the IVD, which is shown in this study. Also, dynamic compressive loading can promote solute transport in the IVD [55]. By taking advantage of IVD mechanical loading conditions, such load-enhanced transport mechanism may further promote nutrient delivery via implanted deformable permeable passive mass transfer devices. Therefore, with proper mechanical and transport properties, the PU mass transfer device could prevent detrimental changes in mechanical environment of IVD cells due to defect and also facilitate nutrient supply to maintain the biological function of IVD cells.

Previous studies have shown promising results in the biological treatments in degenerated disc such as with cell transplantation or with the injection of growth factors [56–60]. However, most of the previous studies used small animals which cannot simulate the conditions of nutrient loss in degenerated human IVDs. The main purpose of the biological treatments (e.g., injection of growth factors and/or cells) is to promote ECM production and to increase cell proliferation [61, 62]. Therefore, the biological treatments will increase the demand for nutrients and worsen the conditions of nutrient loss or low ATP concentration in the disc or NP. The mass transfer device can be used to provide additional nutrient supply

during novel biological treatments. Hence, utilizing PU mass transfer devices may help supplement the biological treatments for degenerated discs to achieve successful outcomes.

One of the limitations in the current study is that only the compressive stiffness was evaluated for the mechanical function of the IVD. Since bending and twisting also are two important motions to spine segments, further experiments are needed to investigate the tensile and torsional biomechanical behaviors. In addition, since the biomechanical and biochemical responses of healthy and degenerated discs to needle punctures may be different, the findings of this study need to be further verified with degenerated discs. Furthermore, distribution of nutrients in the disc was size dependent. To have a consistency of disc size, only three FSUs from L2 to L5 were utilized for the experiments. It limits the number of control groups in our study. Different control groups such as with implantation of non-porous devices or without bone cement sealing will be considered in our future studies. The implantation site of PU mass transfer device was from the dorsal side of AF region which is similar to the location of entry through the AF during the lumbar discogram procedure. One could use a percutaneous procedure similar to a discogram to insert the PU mass transfer devices through the dorsal AF in discs demonstrating degeneration to attempt to arrest disc degeneration from nutrient loss. During daily living, the human lumbar spine withstands compressive loads of high magnitudes [63] which may cause migration and deformation of implanted devices [29]. In this study, no static or dynamic loading was applied to FSUs during 7 days of culture. Therefore, future long term studies are needed to examine the effects of physiological compressive loading on PU mass transfer devices as well as potential integration between tissue and device.

Conclusion

In summary, this study demonstrated the enhancement of energy (ATP) and ECM production in the IVD by utilizing the PU mass transfer devices. In addition, the compressive stiffness and height of the IVD were not affected by implantation of PU mass transfer devices after 7 days of culture. Placing the PU mass transfer device helped to slow loss of disc height when compared to the surgical groups with AF defects only. The results of this study will help in the development of novel treatment strategies for disc degeneration.

Acknowledgments

This study was supported by the grant AR066240 from the NIH and the University of Miami Provost’s Research Award.

References

1. Andersson GBJ. Epidemiological features of chronic low-back pain. Lancet. 1999; 354(9178):581–585. [PubMed: 10470716]
2. Katz JN. Lumbar disc disorders and low-back pain: Socioeconomic factors and consequences. J Bone Joint Surg Am. 2006; 88a:21–24.
3. Smith LJ, Nerurkar NL, Choi KS, Harfe BD, Elliott DM. Degeneration and regeneration of the intervertebral disc: lessons from development. Dis Model Mech. 2011; 4(1):31–41. [PubMed: 21123625]

4. Gilson A, Dreger M, Urban JPG. Differential expression level of cytokeratin 8 in cells of the bovine nucleus pulposus complicates the search for specific intervertebral disc cell markers. Arthritis Res Ther. 2010; 12(1)
5. Adams MA, Roughley PJ. What is intervertebral disc degeneration, and what causes it? Spine. 2006; 31(18):2151–2161. [PubMed: 16915105]
6. Gawri R, Mwale F, Ouellet J, Roughley PJ, Steffen T, Antoniou J, Haglund L. Development of an Organ Culture System for Long-Term Survival of the Intact Human Intervertebral Disc. Spine. 2011; 36(22):1835–1842. [PubMed: 21270705]
7. Pattappa G, Li Z, Peroglio M, Wismer N, Alini M, Grad S. Diversity of intervertebral disc cells: phenotype and function. J Anat. 2012; 221(6):480–496. [PubMed: 22686699]
8. Urban JPG, Roberts S. Degeneration of the intervertebral disc. Arthritis Res Ther. 2003; 5(3):120–130. [PubMed: 12723977]
9. Horner HA, Urban JPG. 2001 Volvo Award winner in basic science studies: Effect of nutrient supply on the viability of cells from the nucleus pulposus of the intervertebral disc. Spine. 2001; 26(23): 2543–2549. [PubMed: 11725234]
10. Boubriak OA, Watson N, Sivan SS, Stubbens N, Urban JP. Factors regulating viable cell density in the intervertebral disc: blood supply in relation to disc height. J Anat. 2013; 222(3):341–8. [PubMed: 23311982]
11. Neidlinger-Wilke C, Mietsch A, Rinkler C, Wilke HJ, Ignatius A, Urban J. Interactions of environmental conditions and mechanical loads have influence on matrix turnover by nucleus pulposus cells. J Orthop Res. 2012; 30(1):112–21. [PubMed: 21674606]
12. Grunhagen T, Shirazi-Adl A, Fairbank JC, Urban JP. Intervertebral disk nutrition: a review of factors influencing concentrations of nutrients and metabolites. Orthop Clin North Am. 2011; 42(4):465–77. vii. [PubMed: 21944584]
13. Zhou S, Cui Z, Urban JP. Nutrient gradients in engineered cartilage: metabolic kinetics measurement and mass transfer modeling. Biotechnol Bioeng. 2008; 101(2):408–21. [PubMed: 18727036]
14. Bibby SR, Jones DA, Ripley RM, Urban JP. Metabolism of the intervertebral disc: effects of low levels of oxygen, glucose, and pH on rates of energy metabolism of bovine nucleus pulposus cells. Spine (Phila Pa 1976). 2005; 30(5):487–96. [PubMed: 15738779]
15. Grunhagen T, Wilde G, Soukane DM, Shirazi-Adl SA, Urban JP. Nutrient supply and intervertebral disc metabolism. J Bone Joint Surg Am. 2006; 88(Suppl 2):30–5. [PubMed: 16595440]
16. An HS, Anderson PA, Haughton VM, Iatridis JC, Kang JD, Lotz JC, Natarajan RN, Oegema TR Jr, Roughley P, Setton LA, Urban JP, Videman T, Andersson GB, Weinstein JN. Introduction: disc degeneration: summary. Spine (Phila Pa 1976). 2004; 29(23):2677–8. [PubMed: 15564916]
17. Huang YC, Urban JPG, Luk KDK. OPINION Intervertebral disc regeneration: do nutrients lead the way? Nat Rev Rheumatol. 2014; 10(9):561–566. [PubMed: 24914695]
18. Urban JPG, Smith S, Fairbank JCT. Nutrition of the intervertebral disc. Spine. 2004; 29(23):2700–2709. [PubMed: 15564919]
19. Wu YR, Cisewski S, Sachs BL, Yao H. Effect of Cartilage Endplate on Cell Based Disc Regeneration: A Finite Element Analysis. Mol Cell Biomech. 2013; 10(2):159–182. [PubMed: 24015481]
20. Jackson AR, Huang CY, Gu WY. Effect of endplate calcification and mechanical deformation on the distribution of glucose in intervertebral disc: a 3D finite element study. Comput Method Biomec. 2011; 14(2):195–204.
21. Gonzales S, Rodriguez B, Barrera C, Huang CYC. Measurement of ATP-Induced Membrane Potential Changes in IVD Cells. Cell Mol Bioeng. 2014; 7(4):598–606. [PubMed: 25386223]
22. Prydz K, Dalen KT. Synthesis and sorting of proteoglycans - Commentary. J Cell Sci. 2000; 113(2):193–205. [PubMed: 10633071]
23. Hirschberg CB, Robbins PW, Abeijon C. Transporters of nucleotide sugars, ATP, and nucleotide sulfate in the endoplasmic reticulum and Golgi apparatus. Annual review of biochemistry. 1998; 67:49–69.
24. Burnstock G. The past, present and future of purine nucleotides as signalling molecules. Neuropharmacology. 1997; 36(9):1127–1139. [PubMed: 9364468]

25. Croucher LJ, Crawford A, Hatton PV, Russell RGG, Buttle DJ. Extracellular ATP and UTP stimulate cartilage proteoglycan and collagen accumulation in bovine articular chondrocyte pellet cultures. Bba-Mol Basis Dis. 2000; 1502(2):297–306.
26. Waldman SD, Usprech J, Flynn LE, Khan AA. Harnessing the purinergic receptor pathway to develop functional engineered cartilage constructs. Osteoarthr Cartilage. 2010; 18(6):864–872.
27. Wang C, Gonzales S, Levene H, Gu WY, Huang CYC. Energy Metabolism of Intervertebral Disc Under Mechanical Loading. J Orthopaed Res. 2013; 31(11):1733–1738.
28. Gonzales S, Wang C, Levene H, Cheung HS, Huang CYC. ATP promotes extracellular matrix biosynthesis of intervertebral disc cells. Cell Tissue Res. 2015; 359(2):635–642. [PubMed: 25407524]
29. Bron JL, van der Veen AJ, Helder MN, van Royen BJ, Smit TH, Amsterdam STEG, MOVE RI. Biomechanical and in vivo evaluation of experimental closure devices of the annulus fibrosus designed for a goat nucleus replacement model. Eur Spine J. 2010; 19(8):1347–1355. [PubMed: 20401620]
30. Likhitpanichkul M, Dreischarf M, Illien-Junger S, Walter BA, Nukaga T, Long RG, Sakai D, Hecht AC, Iatridis JC. Fibrin-Genipin Adhesive Hydrogel for Annulus Fibrosus Repair: Performance Evaluation with Large Animal Organ Culture, in Situ Biomechanics, and in Vivo Degradation Tests. Eur Cells Mater. 2014; 28:25–38.
31. Long RG, Rotman SG, Hom WW, Assael DJ, Grijpma DW, Iatridis JC. In vitro and biomechanical screening of polyethylene glycol and poly(trimethylene carbonate) block copolymers for annulus fibrosus repair. J Tissue Eng Regen Med. 2016
32. Long RG, Torre OM, Hom WW, Assael DJ, Iatridis JC. Design Requirements for Annulus Fibrosus Repair: Review of Forces, Displacements, and Material Properties of the Intervertebral Disk and a Summary of Candidate Hydrogels for Repair. J Biomech Eng-T Asme. 2016; 138(2)
33. Wang YF, Barrera CM, Dauer EA, Gu W, Andreopoulos F, Huang CC. Systematic characterization of porosity and mass transport and mechanical properties of porous polyurethane scaffolds. J Mech Behav Biomed Mater. 2016; 65:657–664. [PubMed: 27741496]
34. Levene, HB. Analysis of tyrosine-derived novel synthetic polymer scaffold devices for guided tissue regeneration. Rutgers University and the University of Medicine and Dentistry of New Jersey; New Brunswick, NJ: 1999. p. 167
35. Huang CYC, Deitzer MA, Cheung HS. Effects of fibrinolytic inhibitors on chondrogenesis of bone-marrow derived mesenchymal stem cells in fibrin gels. Biomech Model Mechan. 2007; 6(1–2):5–11.
36. Yao H, Justiz MA, Flagler D, Gu WY. Effects of swelling pressure and hydraulic permeability on dynamic compressive behavior of lumbar annulus fibrosus. Ann Biomed Eng. 2002; 30(10):1234–1241. [PubMed: 12540199]
37. Johnson S, Rabinovitch P. Ex vivo imaging of excised tissue using vital dyes and confocal microscopy. Curr Protoc Cytom. 2012; Chapter 9(Unit 9):39.
38. Chida J, Yamane K, Takei T, Kido H. An efficient extraction method for quantitation of adenosine triphosphate in mammalian tissues and cells. Anal Chim Acta. 2012; 727:8–12. [PubMed: 22541816]
39. Fernando HN, Czamanski J, Yuan TY, Gu W, Salahadin A, Huang CY. Mechanical loading affects the energy metabolism of intervertebral disc cells. J Orthop Res. 2011; 29(11):1634–41. [PubMed: 21484859]
40. Martin JA, Martini A, Molinari A, Morgan W, Ramalingam W, Buckwalter JA, McKinley TO. Mitochondrial electron transport and glycolysis are coupled in articular cartilage. Osteoarthr Cartilage. 2012; 20(4):323–329.
41. Johnson K, Jung A, Murphy A, Andreyev A, Dykens J, Terkeltaub R. Mitochondrial oxidative phosphorylation is a downstream regulator of nitric oxide effects on chondrocyte matrix synthesis and mineralization. Arthritis and Rheumatism. 2000; 43(7):1560–1570. [PubMed: 10902761]
42. Johnson K, Svensson CI, Van Etten D, Ghosh SS, Murphy AN, Powell HC, Terkeltaub R. Mediation of spontaneous knee osteoarthritis by progressive chondrocyte ATP depletion in Hartley guinea pigs. Arthritis and Rheumatism. 2004; 50(4):1216–1225. [PubMed: 15077304]

43. Bibby SRS, Jones DA, Ripley RM, Urban JPG. Metabolism of the intervertebral disc: Effects of low levels of oxygen, glucose, and pH on rates of energy metabolism of bovine nucleus pulposus cells. Spine. 2005; 30(5):487–496. [PubMed: 15738779]
44. Guehring T, Wilde G, Sumner M, Grunhagen T, Karney GB, Tirlapur UK, Urban JPG. Notochordal Intervertebral Disc Cells Sensitivity to Nutrient Deprivation. Arthritis and Rheumatism. 2009; 60(4):1026–1034. [PubMed: 19333932]
45. Elliott DM, Yerramalli CS, Beckstein JC, Boxberger JI, Johannessen W, Vresilovic EJ. The effect of relative needle diameter in puncture and sham injection animal models of degeneration. Spine (Phila Pa 1976). 2008; 33(6):588–96. [PubMed: 18344851]
46. Hsieh AH, Hwang D, Ryan DA, Freeman AK, Kim H. Degenerative Anular Changes Induced by Puncture Are Associated With Insufficiency of Disc Biomechanical Function. Spine. 2009; 34(10): 998–1005. [PubMed: 19404174]
47. Sobajima S, Kompel JF, Kim JS, Wallach CJ, Robertson DD, Vogt MT, Kang JD, Gilbertson LG. A slowly progressive and reproducible animal model of intervertebral disc degeneration characterized by MRI, x-ray, and histology. Spine. 2005; 30(1):15–24. [PubMed: 15626975]
48. Korecki CL, Costi JJ, Iatridis JC. Needle puncture injury affects intervertebral disc mechanics and biology in an organ culture model. Spine. 2008; 33(3):235–241. [PubMed: 18303454]
49. MacLean JJ, Lee CR, Grad S, Ito K, Alini M, Iatridis JC. Effects of immobilization and dynamic compression on intervertebral disc cell gene expression in vivo. Spine. 2003; 28(10):973–981. [PubMed: 12768134]
50. Walter BA, Korecki CL, Purmessur D, Roughley PJ, Michalek AJ, Iatridis JC. Complex loading affects intervertebral disc mechanics and biology. Osteoarthritis Cartilage. 2011; 19(8):1011–8. [PubMed: 21549847]
51. Wang DL, Jiang SD, Dai LY. Biologic response of the intervertebral disc to static and dynamic compression in vitro. Spine (Phila Pa 1976). 2007; 32(23):2521–8. [PubMed: 17978649]
52. Gu WY, Yao H. Effects of hydration and fixed charge density on fluid transport in charged hydrated soft tissues. Ann Biomed Eng. 2003; 31(10):1162–1170. [PubMed: 14649490]
53. Michalek AJ, Buckley MR, Bonassar LJ, Cohen I, Iatridis JC. The effects of needle puncture injury on microscale shear strain in the intervertebral disc annulus fibrosus. Spine J. 2010; 10(12):1098–1105. [PubMed: 20971041]
54. Jackson A, Gu W. Transport Properties of Cartilaginous Tissues. Curr Rheumatol Rev. 2009; 5(1): 40. [PubMed: 20126303]
55. Huang CY, Gu WY. Effects of mechanical compression on metabolism and distribution of oxygen and lactate in intervertebral disc. J Biomech. 2008; 41(6):1184–1196. [PubMed: 18374341]
56. Acosta FL, Metz L, Adkisson HD, Liu J, Carruthers-Liebenberg E, Milliman C, Maloney M, Lotz JC. Porcine Intervertebral Disc Repair Using Allogeneic Juvenile Articular Chondrocytes or Mesenchymal Stem Cells. Tissue Eng Pt A. 2011; 17(23–24):3045–3055.
57. Drazin D, Rosner J, Avalos P, Acosta F. Stem cell therapy for degenerative disc disease. Adv Orthop. 2012; (2012):961052. [PubMed: 22593830]
58. Henriksson HB, Svanvik T, Jonsson M, Hagman M, Horn M, Lindahl A, Brisby H. Transplantation of Human Mesenchymal Stems Cells Into Intervertebral Discs in a Xenogeneic Porcine Model. Spine. 2009; 34(2):141–148. [PubMed: 19112334]
59. Masuda K, Oegema TR, An HS. Growth factors and treatment of intervertebral disc degeneration. Spine. 2004; 29(23):2757–2769. [PubMed: 15564925]
60. Feng GJ, Zhao XF, Liu H, Zhang HN, Chen XJ, Shi R, Liu X, Zhao XD, Zhang WL, Wang BY. Transplantation of mesenchymal stem cells and nucleus pulposus cells in a degenerative disc model in rabbits: a comparison of 2 cell types as potential candidates for disc regeneration Laboratory investigation. J Neurosurg-Spine. 2011; 14(3):322–329. [PubMed: 21250814]
61. Osada R, Ohshima H, Ishihara H, Yudoh K, Sakai K, Matsui H, Tsuji H. Autocrine/paracrine mechanism of insulin-like growth factor-1 secretion, and the effect of insulin-like growth factor-1 on proteoglycan synthesis in bovine intervertebral discs. J Orthopaed Res. 1996; 14(5):690–699.
62. Pratsinis H, Kletsas D. PDGF, bFGF and IGF-I stimulate the proliferation of intervertebral disc cells in vitro via the activation of the ERK and Akt signaling pathways. Eur Spine J. 2007; 16(11): 1858–1866. [PubMed: 17763874]

63. Schmidt H, Shirazi-Adl A, Galbusera F, Wilke HJ. Response analysis of the lumbar spine during regular daily activities--a finite element analysis. J Biomech. 2010; 43(10):1849–56. [PubMed: 20394933]

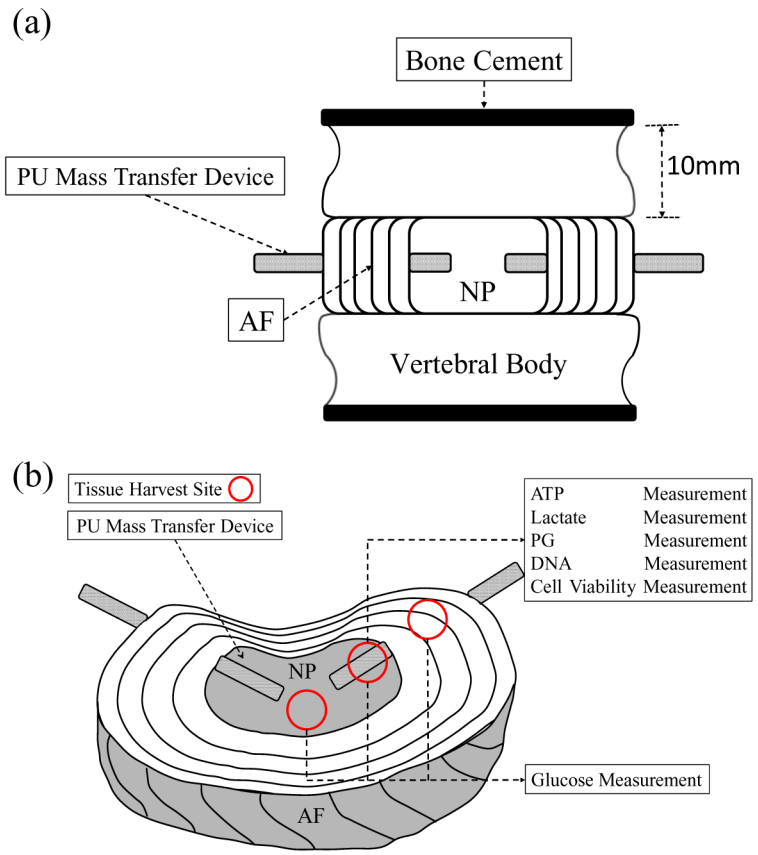

Figure 1.

(a) Schematic of FSU preparation with PU mass transfer device. (b) Locations of PU mass transfer devices implantation and tissue harvest sites including central NP, peripheral NP and AF regions.

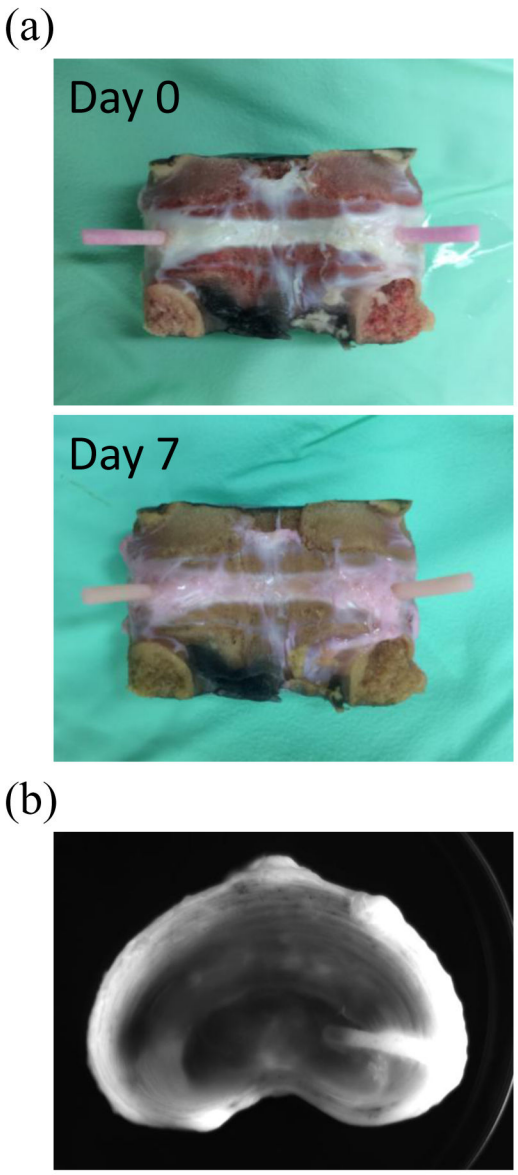

Figure 2.
(a) The typical image of tissue-device boundary at day 0 and day 7. (b) The typical fluorescence image of the mid-height cross section of the IVD from day 0 after 36 hours of incubation with PBS containing Fluorescein.

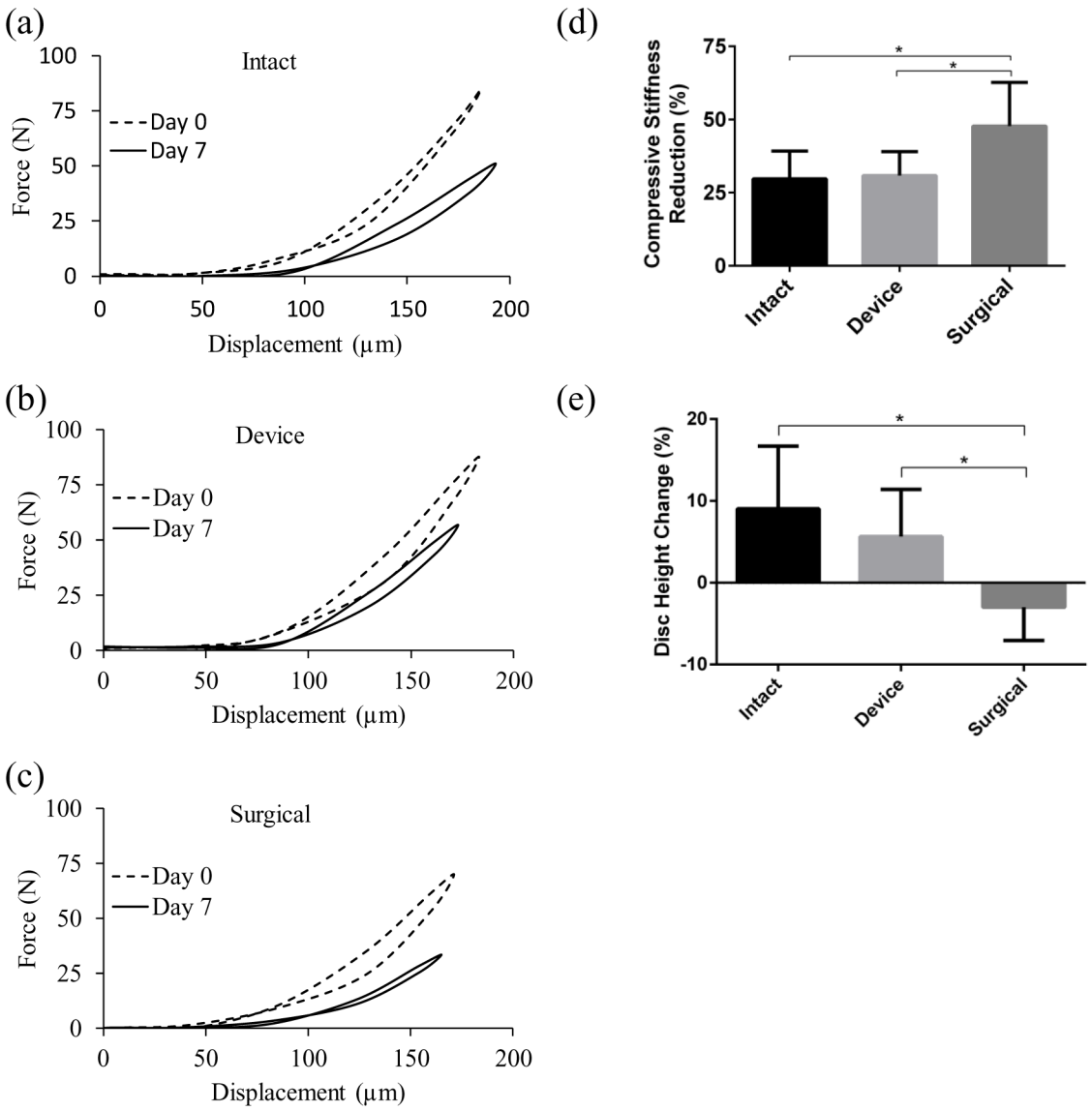

Figure 3.

The typical force-displacement curves from the compressive tests of (a) intact, (b) device and (c) surgical groups. Comparison of (d) compressive stiffness reduction and (e) disc height change among the experimental groups. (* indicate p-value <0.05)

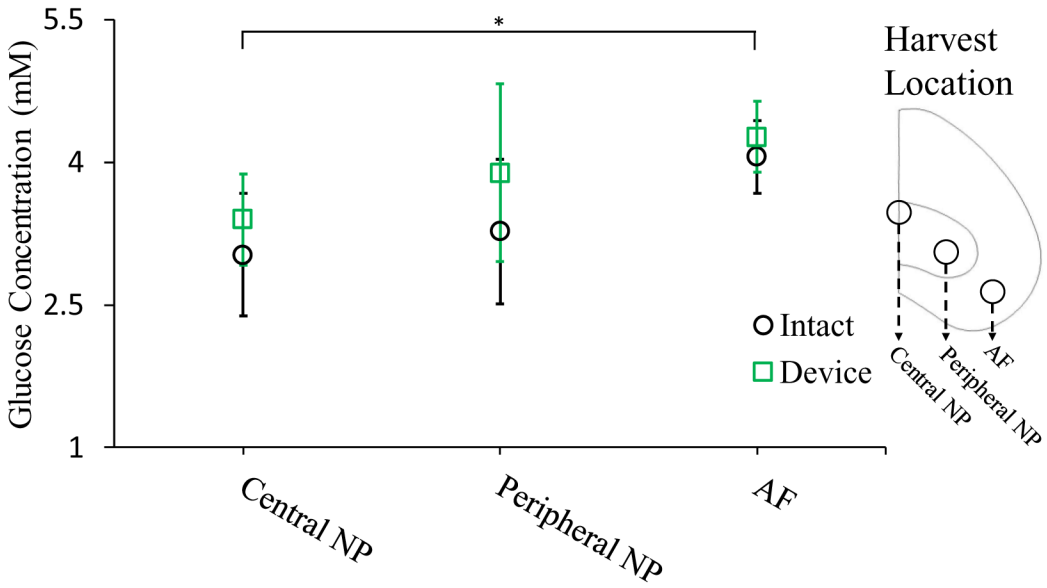

Figure 4.
Comparison of the glucose concentration at central NP, peripheral NP and the AF regions between the intact and device groups. (* indicate p-value <0.05)

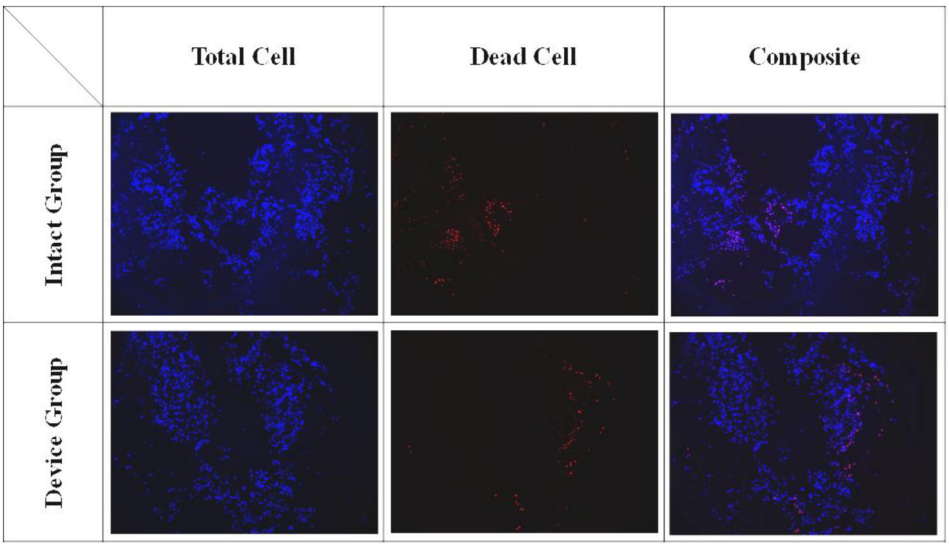

Figure 5.
The typical cell staining of the intact and device groups.

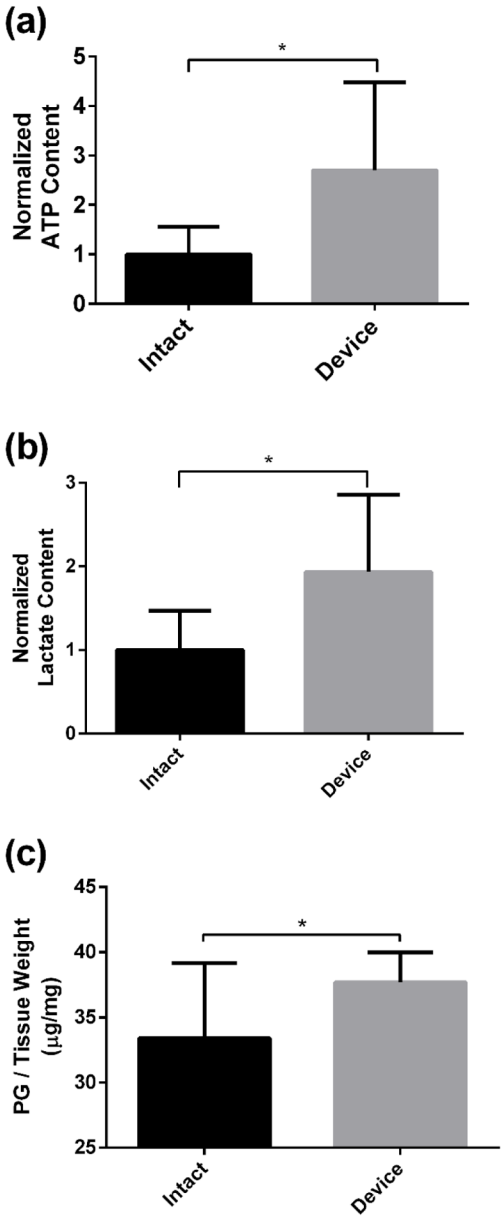

Figure 6.
Comparison of the (a) ATP, (b) lactate and (c) PG contents between the intact and device groups. (* indicate p-value <0.05)

Table 1

The compressive stiffness of the porcine IVD from the intact, device and surgical groups at day 0 and 7.

Compressive Stiffness (N/μm)	Day 0	Day 7
Intact	1406.2 ± 555.1	959.8 ± 315.4
Device	1440.6 ± 500.4	977.6 ± 343
Surgical	1292.4 ± 518.1	650.9 ± 236.6